[Article] Quality by design in the secondary drying step of a freeze-drying process

This is an Accepted Manuscript of an article published by Taylor & Francis Group in *Drying Technology* on 17/08/2012 (Volume 30, Issue 11-12, pages 1307-1313, 2012), available online: http://www.tandfonline.com/doi/abs/10.1080/07373937.2012.704466.

Quality by design in the secondary drying step of a freeze-drying process

Roberto Pisano, Davide Fissore, Antonello A. Barresi

Dipartimento di Scienza Applicata e Tecnologia,

Politecnico di Torino, corso Duca degli Abruzzi 24, 10129 Torino (Italy)

Abstract

This paper is focused on the secondary drying step of a freeze-drying process, where the bound water is desorbed from the (partially) dried product, with the goal to achieve the target value of residual moisture in the final product.

Mathematical modeling is used to get a deep understanding of the process, i.e. to study the effect of the operating variables (mainly the temperature of the heating shelf and the duration of the operation) on the state of the product (temperature and residual moisture).

An innovative tool is used to provide an effective support to get quality by design: it is based on the measurement of the desorption rate, through the test of pressure rise, and on a mathematical model of the process. It allows to monitor in-line the process, as well as to determine the kinetic parameters of water desorption, and their dependence on the operating conditions.

The mathematical model of the process is used to build the design space of the secondary drying process, i.e. to identify those operating conditions that allow to fulfill product quality requirements, and then to minimize the duration of the secondary drying.

The case study used to test the proposed methodology is the drying of 5% w/w aqueous solutions of sucrose: a linear dependence of the desorption rate on the residual moisture is evidenced by the experimental investigation, and the Arrhenius equation appears to adequately describe the dependence of the kinetic constant on the temperature, with a frequency factor equal to 277 s^{-1}, and an activation energy equal to 37,714 J mol^{-1}. The model is then used to calculate the design space, as well as to optimize the operating conditions: in case the target value of residual moisture is 2% the duration of secondary drying can be decreased from 16 h in case of constant shelf temperature to 7.35 h in case the recipe is optimized.

Key words

Freeze-drying; Pharmaceuticals; Secondary drying; Quality by design; Mathematical model.

Introduction

In recent years quality by design has become the leading paradigm in pharmaceuticals manufacturing, with the goal to improve product quality and make processes more efficient and cost-effective. This is particularly true for the freeze-drying process, a key step in many biologicals and biopharmaceuticals manufacturing processes as it allows recovering the active pharmaceutical ingredient from a solution at low temperature and in sterile conditions. As a consequence, freeze-drying is used in case of temperature sensitive products.[1-5] A great deal of work has been done to optimize in-line[6-15], or off-line[16-26], the primary drying step, where the ice sublimation occurs, and valuable methods have been proposed and validated to preserve product quality, beside speeding up the process.

As not all of the water freezes during the freezing stage, but a certain amount remains bound to the product, a further step is required to achieve the target value of the residual moisture in the final product. During the secondary drying step, the desorption of the bound water takes place.

The typical procedure consists of rising the shelf temperature up to a value that does not jeopardize product properties, and maintaining the product at the selected temperature for several hours. Generally, shelf temperature is set equal to 25°C or higher values, which is generally higher than the value used during primary drying.[27] A very low value of chamber pressure is generally used to carry out the secondary drying, even if there are no evidences in the Literature that this could provide any advantage when pharmaceuticals are processed. Moreover, a very low value of chamber pressure can cause the transfer of volatile stopper components to the product.[28] In the phase of recipe design various samples can be periodically taken from the drying chamber (e.g. with a "sample thief") with the goal to measure off-line their moisture content, by means of Karl Fischer titration, gravimetric analysis[6], or NIR spectroscopy[29]. By this way it is possible to determine when the target value of residual moisture is obtained and, thus, the duration of the secondary drying phase.

Few rationalization attempts were carried out in the past. Pikal et al.[30] proposed simple heuristics for the selection of the heating shelf temperature and of the drying duration in case of crystalline and non-crystalline formulations: in the first case secondary drying is initially carried out at 40°C, and then the temperature of the heating shelf is increased to 50°C, while in the second case shelf temperature should be kept constant (and equal to 40°C) for a time interval that depends on the solid concentration. The shelf temperature can then be modified on the basis of the value of residual moisture, in case this value is measured (or estimated),

and simple heuristics are given to this purpose. This method can be really useful to set the operating conditions of the secondary drying phase as it does not require any information about the product, but the recipe is evidently far from being optimized, and it is not possible to control the moisture content in the final product.

Mayeresse[31] proposed a simple non-linear equation, based on a suitable design-of-experiment, that allows to predict the final moisture as a function of process parameters (shelf temperature and time) for a specific product with a specific product concentration. Despite the fact that this type of statistical modeling can be worthwhile to determine the operating conditions for the desired final moisture level, the method requires a huge amount of experiments, the results are product dependent, and it is not possible to extrapolate data outside the tested values.

In this paper a simple mathematical model is proposed to describe the effect of the operating variables on the state of the product, i.e. on the temperature and residual moisture. The structure of the paper is the following: at first model equations are presented, as well as model parameters and the techniques that could be used to determine their values experimentally. Then, it is described the procedure used to calculate the design space for the secondary drying, i.e. to identify those operating conditions that allow to fulfill product quality requirements. Finally, the possibility of using mathematical modeling to identify the "best" operating conditions, i.e. to minimize the duration of the secondary drying, is addressed.

Methods and Materials

Process model

A simple lumped model can be used to describe the evolution of the product temperature and of the amount of residual moisture *vs*. time during secondary drying. Both radial and axial gradients of temperature and concentration are assumed to be negligible and, thus, the energy balance for the product contained in the vial is given by the following equation:

$$\rho_p c_{p,p} V_p \frac{dT_p}{dt} = K_v A_v \left(T_{\text{fluid}} - T_p\right) + V_p \rho_p r_d \Delta H_{\text{des}} \qquad (1)$$

where T_{fluid} is the temperature of the fluid that circulates in the shelves of the freeze-dryer, and the mass balance is simply given by the following equation:

$$\frac{dC_s}{dt} = -r_d \quad (2)$$

where r_d is the water desorption rate per unit of mass.

Model equations can be solved in case other two parameters, that can be easily determined by means of few experiments, are known, beside some physico-chemical parameters, namely;

i. the overall heat transfer coefficient from the heating shelf to the product in the container (K_v);
ii. the kinetic parameters used to model the dependence of the water desorption rate on the residual moisture concentration and on the temperature of the product

The parameter K_v is an effective heat transfer coefficient that takes into account all the heat transfer mechanisms to the product, namely[19,21,32,33]:

i. conduction in the contact points between the shelf (or the tray, in case it is used to load the vials in the freeze-dryer) and the vial;
ii. conduction in the gas contained in the gap between the vial bottom and the shelf (or tray);
iii. radiation from the shelf and from chamber walls (in the case the vial is placed at the edges of the shelf, in front of chamber walls);
iv. conduction from the metal frame that is sometimes used to load vials onto the shelves.

The value of K_v is dependent on chamber pressure, and it can be described by the following equation:

$$K_v = C_1 + \frac{C_2 P_c}{1 + C_3 P_c} \quad (3)$$

The coefficients C_1, C_2 and C_3 depends on the vial-dryer system and on the position of the vial on the shelves.

The kinetics of water removal (from an amorphous solid) is dependent on:

i. molecular diffusion of water in the glassy solid from the interior of a particle to the surface;
ii. evaporation at the solid-vapor interface;
iii. water vapor transport through the porous dried cake;
iv. water vapor transport from the headspace in the vial to the condenser.

Extensive investigations carried out by Pikal et al.[27] with crystalline (mannitol) and amorphous (moxalactam di-sodium and povidone) products evidenced that the vapor transport in the dried cake is generally not the limiting factor. In fact, there is no significant effect of dried cake thickness on drying rate, and there is almost no effect of chamber pressure on

drying rate, while a higher drying rate is observed in case the specific surface area is increased. As neither the apparatus, nor the pore systems of the dried cake appear to be rate limiting for secondary drying, it is assumed that the rate-determining step is water desorption from the solid.

Various equations were proposed in the past to model the dependence of r_d on residual moisture, assuming that the desorption rate is proportional either to residual moisture:

$$r_d = ak_d C_s \tag{4}$$

or to the difference between residual moisture and the equilibrium value:

$$r_d = ak_d \left(C_s - C_{s,\mathrm{eq}} \right) \tag{5}$$

where a is the specific surface of the product.[34,35] Even if either diffusion in the solid matrix or desorption from solid surface could be the controlling mechanism[27], and this can be affected by the physical state of the product (crystalline or amorphous), equations (4) and (5) can be used in any case to describe the phenomenon, even if the parameter k_d assumes a slightly different physical meaning. Equation (4) will be used in the following as it is much simpler (and it does not require to know the values of $C_{s,\mathrm{eq}}$), and it has been demonstrated to describe adequately the process[18]. In any case, the adequacy of such hypothesis can be easily tested by means of few experiments, and a different model can be used to account for the dependence of the desorption rate on residual moisture instead of equation (4)..

The kinetic constant k_d is dependent on product temperature according to an Arrhenius-type equation:

$$k_d = k_{d,0} \exp\left(-\frac{E_{a,d}}{\mathrm{R}T_p} \right) \tag{6}$$

Also this hypothesis can be easily tested experimentally. The effect of chamber pressure on drying kinetics, according to previous papers (see Refs. [27], [36]) is assumed to be negligible, at least in the range 0-20 Pa (higher values of chamber pressure are generally avoided as they can make the vapor flow through the pore structure the rate limiting step, thus causing a significant decrease of the drying rate).

Determination of model parameters

The overall heat transfer coefficient can be determined experimentally by means of various methods:

i. Gravimetric test: a batch of vials, filled with water (or with the solution containing the active pharmaceutical ingredient) is frozen and, then, ice sublimates for a time interval

(Δt), thus causing a weight loss (Δm) that has to be measured in each vial using an analytical balance. The temperature of the ice at the vial bottom (T_B) has also to be measured, and the coefficient K_v is calculated by means of the following equation:

$$K_v = \frac{\Delta m \cdot \Delta H_s}{A_v \cdot \int_0^{\Delta t} (T_{\text{fluid}} - T_B) dt} = \frac{\bar{J}_w \cdot \Delta t \cdot \Delta H_s}{A_v \cdot \int_0^{\Delta t} (T_{\text{fluid}} - T_B) dt} \quad (7)$$

ii. The Tunable Diode Laser Absorption Spectroscopy can be used to determine the sublimation flux J_w and, if T_B is also measured, equation (7) can be used to calculate K_v.[37-39]

iii. The pressure rise test (PRT) can be used to determine K_v: the valve in the duct between the drying chamber and the condenser is closed for few seconds, and various parameters (e.g. K_v) are retrieved looking for the best fit between the calculated and the measured values of pressure rise.[40-44]

While methods (ii) and (iii) gives a "mean", or effective, value of K_v for all the vials of the batch, the gravimetric test allows to take into account the non-uniformity of the batch and, thus, it will be used in this study. The test has to be carried out at the same value of chamber pressure used in the secondary drying phase; in case chamber pressure is modified during secondary drying, the parameters appearing in equation (3) have to be determined and, thus, at least three different tests, each of them carried out at a different value of chamber pressure, are required, looking for the best fit between the measured and the calculated values of K_v.

With respect to the kinetic constant of the desorption reaction, the soft-sensor recently proposed by the authors has been used.[45,46] It is based on the measurement of the desorption rate from the curve of pressure rise during the PRT:

$$r_{d,\text{PRT}} = 100 \cdot \frac{\frac{M_w V_c}{\text{R} T_c} \left. \frac{dP_c}{dt} \right|_{t=t_{0,PRT}}}{m_{\text{dried}}} \quad (8)$$

and on a mathematical model describing the water desorption from the product (equations (2) and (4)). The value of the residual moisture in the product at the beginning of secondary drying ($C_{s,0}$) and of the kinetic constant k_d are obtained looking for the best fit between the measured and the calculated values of desorption rate.

Off-line recipe design and optimization

The design space can be defined as the set of operating conditions (temperature of the heating

fluid and duration of the secondary drying) that allows to get the target value of residual moisture in the product, taking into account the maximum temperature allowed by the product. This requires to know how the glass transition temperature changes as a function of the residual moisture content in the product. In case of sucrose solutions a simplified version of the Gordon-Taylor equation proposed by Hancock and Zografi[47] can be used:

$$T_g = \frac{C_s T_{g,w} + K\left(1-C_s\right)T_{g,s}}{C_s + K\left(1-C_s\right)} \quad (9)$$

with K = 0.2721, $T_{g,w}$ = 135 K and $T_{g,s}$ = 347 K. The following procedure can be used to calculate the design space for the secondary drying phase:

i. Selection of the vector of values of T_{fluid} of interest, where $T_{\text{fluid},i}$ is the i-th value of fluid temperature.
ii. Calculation of the maximum allowed value of product temperature as a function of the residual moisture content (using eq. (9)).
iii. Selection of the value of $C_{s,0}$.
iv. Calculation of the evolution of T_p and C_s, using the model of the process, for the i-th value of fluid temperature $T_{\text{fluid},i}$.
v. Determination of the time ($t_{d,i}$) required to get the target value of residual moisture ($C_{s,t}$) when $T_{\text{fluid}} = T_{\text{fluid},i}$.
vi. The couple of values ($t_{d,i}$, $T_{\text{fluid},i}$) belongs to the design space in case product temperature remains below the limit value throughout the drying phase.
vii. Repetition of steps (iv)-(vi) for all the values of $T_{\text{fluid},i}$ of interest.
viii. Repetition of steps (iv)-(vii) for different values of $C_{s,0}$ as this variable can be hardly known, and it can be not the same for the various vials of the batch (this issue will be discussed in the following section).

Using the design space it is thus possible to optimize the secondary drying by selecting the value of T_{fluid} that allows minimizing t_d.

The process can be further optimized by looking for a much more "aggressive" control policy, using different set-points for the fluid temperature during secondary drying, in such a way that product temperature is always close to the limit value as drying goes on (and the limit temperature increases). Examples of such calculations will be shown in the following section.

Case study and experimental methods

The case study used to test the proposed methodology for design space calculation and recipe

optimization is the drying of 5% w/w aqueous solutions of sucrose (Riedel de Haën, highest analytical grade). Solutions were prepared using ultra-pure water (Milli-Q RG, Millipore, Billerica, MA) and processed into ISO 8362-1 2R tubing vials (internal diameter = 14.25 mm), filled with 1.5 mL of solution. Vials are loaded directly on the shelf and they are arranged in clusters of hexagonal arrays, surrounded by a metal frame. The process is carried out in a pilot-scale freeze-dryer (LyoBeta 25 by Telstar, Spain) with a chamber volume of 0.2 m^3 and equipped with capacitance (Baratron type 626A, by MKS Instruments, Andover, MA, USA) and thermal conductivity (Pirani type PSG-101-S, by Inficon, Bad Ragaz, Switzerland) gauges. The pressure in the drying chamber is regulated by bleeding of inert gas. The end of primary drying is estimated using the ratio of Pirani and Baratron sensors.[48,49] Product temperature at the bottom of the vials is measured using T-type miniature thermocouples (Tersid, Milano, Italy).

In the tests used to determine the parameter K_v, each vial of the batch was filled with 2 mL of ultra-pure water, and ice sublimation was carried out for 6 h. The set point for the heating fluid temperature was equal to -15°C, and three different tests were carried out, being chamber pressure equal to 5, 15, and 25 Pa respectively, in order to determine the parameters of eq. (3) using the procedure described in the previous section.

In the runs used to determine the kinetic model of the desorption reaction, and the dependence of the kinetic constant on product temperature, as well as in the tests carried out for model validation purposes, the desorption flux was measured using the PRT, while the residual moisture in some vials extracted from the drying chamber using a sample thief was measured by Karl Fischer titration (using a Compact Karl Fischer Coulometer, by Mettler Toledo, Columbia, OH, USA). In these tests primary drying was carried out at 5 Pa, and the set-point temperature for the heating fluid was equal to -10°C, while secondary drying was carried out using different set-points for T_{fluid} (in different runs) in order to evaluate the dependence of k_d on T_p, while the pressure in the drying chamber was about 5 Pa.

Results and discussion

In order to use the mathematical model (equations (1)-(2)) for calculating the design space and optimizing secondary drying it is firstly necessary to determine the parameters of the model, namely K_v and k_d. The overall heat transfer coefficient has been determined according to the procedure described in the previous section. Results obtained when P_c = 5 Pa are shown

in Figure 1. It appears that the value of K_v is not the same for all the vials of the batch as this parameter is, actually, an effective coefficient, that takes into account all the heat transfer mechanisms to the product. Thus, in case the product in the vials is heated only by the shelf, as in the vials in the centre of the batch, the value of K_v is lower than that obtained from vials at the edges of the shelf, where the product is heated also by radiation from chamber walls, and by conduction from the metal frame used to load-unload the vials. With this respect we identified 4 groups of vials, characterized by a different position over the shelf, and by different additional heat transfer mechanisms (Table 1). This test was then repeated for other two values of chamber pressure, and, finally, the values of C_1, C_2, and C_3 required to model the dependence of K_v on P_c were calculated. Results are given in Table 1 for the 4 groups of vials (it can be highlighted that only the value of C_1 changes according to the group of vials, while the parameters C_2, and C_3 have the same values for all the vials, as the latter express the dependence of the parameter on chamber pressure, that is evidently the same for all the vials, independently on their position over the shelf, while the former express the contribution of conduction and radiation to heat transfer).

With respect to the kinetic constant k_d we need firstly to verify the hypothesis of linear dependence of the desorption rate on the residual moisture (eq. (4)) and of Arrhenius-type dependence of k_d on product temperature (eq. (6)). Three tests have been carried out with different set-point of the heating fluid temperature: in the first part of the secondary drying the temperature of the heating shelf rises from the value used during primary drying (-10°C) to the target value, and then it remains constant. The desorption rate is measured using the test of pressure rise and the results are shown in Figure 2. The soft-sensor designed by the authors to monitor secondary drying[45,46] is then used to determine k_d.

Figure 3 (graph A) shows the dependence of r_d on C_s, thus proving that a linear equation like eq. (4) is suitable to model this dependence for the three tests that have been carried out. The determination coefficient (R^2) can be used to check the adequacy of the linear model: its value range from 0.90, when the heating fluid temperature is 20°C, to 0.99 when the heating fluid temperature is 40°C, thus proving the adequacy of the hypothesis. The Arrhenius plot is then shown in Figure 3 (graph B), pointing out that eq. (6) is able to model the dependence of k_d on T_p. In this case the determination coefficient is 0.89. In this case $a\ k_{d,0}$ is equal to 277 s^{-1}, while the activation energy ($E_{a,d}$) is equal to 37,714 J mol^{-1}.

At this point model validation can be carried out. Figure 4 shows an example of the results obtained in one of the various tests that were run at different operating conditions. The calculated values of desorption rate are compared with those measured using the test of

pressure rise, while the calculated values of residual moisture in the product are compared with the values obtained extracting vials from the chamber, and using Karl Fisher Titration. Finally, the calculated product temperature is compared with the values obtained through the T-type thermocouple inserted in some vials. In all cases the agreement between measured and calculated values is particularly good and satisfactory.

Once the model of the process has been validated, it can be used to calculate the design space. An example of this calculation is shown in Figure 5 (graph A) for the vials of group 4, i.e. those in the central position over the shelf. In this case the maximum fluid temperature is assumed to be equal to 40°C and, for a target value of residual moisture (e.g. 2%) the design space is coincident with the area of the diagram below the solid line. Dashed line corresponds to operating conditions for which the limit value of product temperature is trespassed and, thus, they do not belong to the design space. In case the target value of residual moisture ranges between two values, e.g. 1 and 2%, then the design space corresponds to the area comprised between the two curves that are the boundaries of the design spaces calculated for $C_{s,t}$ = 1% and 2% respectively (Figure 5, graph B).

It has to be highlighted that in order to calculate the design space we need to know the value of $C_{s,0}$, i.e. of the residual moisture in the product at the end of primary drying (i.e. at the beginning of secondary drying). Actually, a large non-uniformity can exist among the vials of the batch with respect to this value, as it can be seen from Figure 6, where the distribution of the values of $C_{s,0}$ in one test is shown (it was determined by stopping the process at the end of primary drying, and calculating the residual moisture from the weight loss in the vials of the batch). The effect of $C_{s,0}$ on the design space can be easily determined (it is sufficient to calculate various design spaces, one for each values of $C_{s,0}$) as it appears from Figure 7 (graph A), where three design spaces calculated for three different values of $C_{s,0}$ are shown. This allows the user to identify the couple of values of fluid temperature and secondary drying duration that allow to get the target value of residual moisture in the most critical vials, i.e. those with the highest initial value of residual moisture.

Beside the value of $C_{s,0}$, also the overall heat transfer coefficient K_v is not the same for all the vials of the batch as it depends on the position of the vial over the shelf. It is again very easy to calculate the design space for different values of K_v: an example of these calculations is shown in Figure 7 (graph B), where it appears that the parameter K_v has a poor influence on the design space.

Using the design spaces shown in Figures 5 and 7 it is possible to optimize the secondary drying by selecting the value of fluid temperature that minimizes the duration of

the desorption step, taking into account the constraint on maximum product temperature. A further optimization can be carried out using various set-points for the fluid temperature during secondary drying, in such a way that product temperature is always as close as possible to the limit value. In fact, as drying goes on, and the residual moisture concentration decreases, the limit temperature increases. Figure 8 shows an example of this calculation: in this case the temperature of the heating fluid has been modified every hour, and the new set-point value was set to 1 K below the limit product temperature (calculated for the value of the residual moisture at that time). Figure 8 (graph A) shows how the limit temperature increases with time: product temperature, that remains (obviously) below the temperature of the heating fluid, never trespasses the limit value. The evolutions of the desorption rate and of the residual moisture are shown in graphs B and C respectively.

It is evidently possible to use different heating strategies: Figure 9 compares the results obtained when fluid temperature is maintained constant, when it is changed after eight hours, and when it is changed every hour. Evidently, in case the heating policy is much more "aggressive", the drying time can be significantly reduced: for the case study shown in Figure 9, in case $C_{s,t}$ = 2% the duration of secondary drying changes from 16 h in case of constant $T_{\mathrm{fluid,sp}}$, to 7.35 h in case the set point of fluid temperature is modified every hour.

Conclusions

Secondary drying is an important step in all freeze-drying processes; nevertheless, the operating conditions for a certain product are generally set by trial and error, or in analogy with those used for other products. As a result the process is not optimized, and the duration can be as long as that of the primary drying phase. This arises also from the lack of knowledge about the process, due to the difficulty of measuring the evolution of the residual moisture in the product without extracting vials from the chamber.

The availability of a new soft-sensor providing reliable estimations of the residual moisture content in the product during secondary drying allows to set up a true quality by design framework. A simple mathematical model of the process has been shown to be useful to calculate the design space of the process, as well as to minimize its duration beside fulfilling the constraint on maximum product temperature, and obtaining the target value of residual moisture. Moreover, the proposed method can be used both in small-scale and in industrial-scale freeze-dryers, with a really small experimental (and computational) effort.

Acknowledgements

The contribution of Daniele Sorce for the experimental investigation is gratefully acknowledged.

List of Symbols

A_v	cross sectional area of the vial, m^2
a	specific surface of the dried product, m^2 $kg^{-1}_{\text{dried product}}$
C_1	parameter used in eq. (3), W K^{-1} m^{-2}
C_2	parameter used in eq. (3), W $K^{-1}m^{-2}Pa^{-1}$
C_3	parameter used in eq. (3), Pa^{-1}
C_s	residual moisture, kg_{water} $kg^{-1}_{\text{dried product}}$
$C_{s,0}$	residual moisture at the beginning of secondary drying, kg_{water} $kg^{-1}_{\text{dried product}}$
$C_{s,\text{eq}}$	weight fraction of sorbed water in the solid that would be in local equilibrium with the partial pressure of water in the drying chamber, kg_{water} $kg^{-1}_{\text{dried product}}$
$C_{s,t}$	target value residual moisture at the end of secondary drying, kg_{water} $kg^{-1}_{\text{dried product}}$
$c_{p,p}$	specific heat of the product, J $kg^{-1}K^{-1}$
$E_{a,d}$	activation energy of the desorption reaction, J mol^{-1}
ΔH_{des}	heat of desorption, J kg^{-1}_{water}
ΔH_s	heat of sublimation, J kg^{-1}_{water}
$\bar{J}_w$	mean value of the solvent sublimation flux, kg $m^{-2}s^{-1}$
K	parameter used in eq. (9)
K_v	overall heat transfer coefficient, W $K^{-1}m^{-2}$
k_d	kinetic constant of the desorption rate, $kg^{-1}_{\text{dried product}}$ s^{-1} m^{-2}
$k_{d,0}$	pre-exponential factor of the kinetic constant of the desorption rate, $kg^{-1}_{\text{dried product}}$ s^{-1} m^{-2}
M_w	solvent molar mass, kg mol^{-1}
m	mass, kg
m_{dried}	mass of dried product, kg
P_c	chamber pressure, Pa
R	ideal gas constant, J $K^{-1}mol^{-1}$
r_d	water desorption rate, kg_{water} $kg^{-1}_{\text{dried product}}$ s^{-1}

$r_{d,\mathrm{PRT}}$	water desorption rate measured through the test of pressure rise, $kg_{water}\ kg^{-1}_{dried\ product}\ s^{-1}$
T_B	product temperature at the bottom of the vial, K
T_c	temperature of the vapor in the drying chamber, K
T_{fluid}	temperature of the heating fluid, K
$T_{\mathrm{fluid,sp}}$	set-point for the temperature of the heating fluid, K
T_g	glass transition temperature, K
$T_{g,s}$	sucrose glass transition temperature, K
$T_{g,w}$	ice glass transition temperature, K
T_p	product temperature, K
t	time, s
$t_{0,\mathrm{PRT}}$	starting point of the PRT, s
t_d	duration of secondary drying, h
V_c	free volume of the chamber, m^3
V_p	volume of the product, m^3

Greeks

ρ_p	apparent density of the product, kg m^{-3}

Abbreviations

PRT	Pressure Rise Test

References

1 Franks, F. *Freeze-drying of pharmaceuticals and biopharmaceuticals*. Royal Society of Chemistry: Cambridge, 2007.

2 Matejtschuk, P.; Malik, K.; Duru, C.; Bristow, A. Freeze drying of biologicals: process development to ensure biostability. American Pharmaceutical Review **2009**, *12*, 54-58.

3 Rathore, A.S.; Winkle, H. Quality by design for biopharmaceuticals. Nature Biotechnology **2009**, *27*, 26-34.

4 Liapis, A.I.; Pikal, M.J.; Bruttini, R. Research and development needs and opportunities in freeze drying. Drying Technology **1996**, *14*, 1265–1300.

5 Sadikoglu, H.; Ozdemir, M.; Seker, M. Freeze-drying of pharmaceutical products: Research and development needs. Drying Technology **2006**, *24*, 849-861.

6 Tang, X.C.; Pikal, M.J. Design of freeze-drying processes for pharmaceuticals: practical advice. Pharmaceutical Research **2004**, *21*,191-200.

7 Tang, X.C.; Nail, S.L.; Pikal, M.J. Freeze-drying process design by manometric temperature measurement: Design of a smart freeze-dryer. Pharmaceutical Research **2005**, *22*, 685-700.

8 Gieseler, H.; Kramer, T.; Pikal, M.J. Use of manometric temperature measurement (MTM) and SMART™ freeze dryer technology for development of an optimized freeze-drying cycle. Journal of Pharmaceutical Sciences **2007**, *96*, 3402-3418.

9 Barresi, A.A.; Velardi, S.A.; Pisano, R.; Rasetto, V.; Vallan, A.; Galan, M. In-line control of the lyophilization process. A gentle PAT approach using software sensors. International Journal of Refrigeration **2009**, *32*, 1003-1014.

10 Fissore, D.; Pisano, R.; Rasetto, V.; Marchisio, D.L.; Barresi, A.A.; Vallan, A.; Corbellini, S. Applying Process Analytical Technology (PAT) to lyophilization processes. Chimica Oggi-Chemistry Today **2009**, *27* (2, Supplement), vii-xi.

11 Barresi, A.A.; Pisano, R.; Rasetto, V.; Fissore, D; Marchisio, D.L. Model-based monitoring and control of industrial freeze-drying processes: effect of batch non-uniformity. Drying Technology **2010**, *28*, 577-590.

12 Fissore, D.; Pisano, R.; Velardi, S.A.; Barresi, A.A.; Galan M. PAT tools for the optimization of the freeze-drying process. Pharmaceutical Engineering **2010**, *29*, 58-70.

13 Pisano, R.; Fissore, D.; Velardi, S.A.; Barresi A.A. In-line optimization and control of an industrial freeze-drying process for pharmaceuticals. Journal of Pharmaceutical Sciences **2010**, *99*, 4691-4709.

14 Daraoui, N.; Dufour, P.; Hammouri, H.; Hottot A. Model predictive control during the primary drying stage of lyophilisation. Control Engineering Practice **2010**, *18*, 483-494.

15 Pisano, R.; Fissore, D.; Barresi, A.A. Freeze-drying cycle optimization using Model Predictive Control techniques. Industrial Engineering Chemistry Research **2011**, *50*, 7363-7379.

16 Lombraña, J.I.; De Elvira, C.; Villaran, M.C.; Izcara, J. Simulation and design of heating profiles in heat controlled freeze-drying of pharmaceuticals in vials by the application of a sublimation semispherical model. Drying Technology **1993**, *11*, 471-487.

17 Lombraña, J.I.; De Elvira, C.; Villaran, M.C.; Izcara, J.. Simulation and design of heating profiles in heat controlled freeze-drying of pharmaceuticals in vials by the application of a sublimation cylindrical model. Drying Technology **1003**, *11*, 85-102.

18 Sadikoglu, H.; Liapis, A.I. Mathematical modelling of the primary and secondary drying stages of bulk solution freeze-drying in trays: parameter estimation and model discrimination by comparison of theoretical results with experimental data. Drying Technology **1997**, *15*, 791-810.

19 Gan, K.H.; Crosser, O.K.; Liapis, A.I.; Bruttini, R. Lyophilisation in vials on trays: effects of tray side. Drying Technology **2005**, *23*, 341-363.

20 Hottot, A.; Peczalski, R.; Vessot, S.; Andrieu, J. Freeze-drying of pharmaceutical proteins in vials: modeling of freezing and sublimation steps. Drying Technology **2006**, *24*, 561-570.

21 Velardi, S.A.; Barresi, A.A. Development of simplified models for the freeze-drying process and investigation of the optimal operating conditions. Chemical Engineering Research and Design **2008**, *86*, 9-22.

22 Brülls, M.; Rasmuson, A. Ice sublimation in vial lyophilization. Drying Technology **2009**, *27*, 695-706.

23 Sundaram, J.; Hsu, C.C.; Shay, Y.M.; Sane, S.U. Design space development for lyophilization using DOE and process modeling. BioPharm International **2010**, *23*, 26-36.

24 Giordano, A.; Barresi, A.A.; Fissore, D. On the use of mathematical models to build the design space for the primary drying phase of a pharmaceutical lyophilization process. Journal of Pharmaceutical Sciences **2011**, *100*, 311-324.

25 Koganti, V.R.; Shalaev, E.Y.; Berry, M.R.; Osterberg, T.; Youssef, M.; Hiebert, D.N.; Kanka, F.A.; Nolan, M.; Barrett, R.; Scalzo, G.; Fitzpatrick, G.; Fitzgibbon, N.; Luthra, S.; Zhang, L. Investigation of design space for freeze-drying: use of modeling for primary drying segment of a freeze-drying cycle. AAPS PharmSciTech **2011**, *12*, 854-861.

26 Fissore, D.; Pisano, R.; Barresi, A.A. Advanced approach to build the design space for the primary drying of a pharmaceutical freeze-drying process. Journal of Pharmaceutical Sciences **2011**, *100*, 4922-4933.

27 Pikal, M.J.; Shah, S.; Roy, M.L.; Putman, R. The secondary drying stage of freeze drying: drying kinetics as a function of temperature and pressure. International Journal of Pharmaceutics **1980**, *60*, 203-217.

28 Pikal, M.J.; Lang, J. E. Rubber closures as a source of haze in freeze-dried parenterals: Test methodology for closure evaluation. Journal of Parenteral Drug Association **1978**, *32*, 162-173.

29 Last, I.R.; Prebble, K.A. Suitability of near-infrared methods for the determination of moisture in a freeze-dried injection product containing different amounts of the active ingredient. Journal of Pharmaceutical and Biomedical Analysis **1993**, *2*, 1071-1076.

30 Pikal, M.J.; Tang, X.C.; Nail, S.L. Automated process control using manometric temperature measurement. United States patent US 6971187 B1, 2005.

31 Mayeresse, Y. Moisture content in freeze-dried product. Cambridge Healthtech Institute's Seventh Annual Pep Talk 2008, January 7-11, San Diego, California.

32 Pikal, M.J. Heat and mass transfer in low pressure gases: applications to freeze-drying. In: *Transport Processes in Pharmaceutical Systems*; Amidon, G.L., Lee, P.I., Topp, E.M., Eds.; Marcel Dekker: New York, 2000; 611-686.

33 Pisano, R.; Fissore, D.; Barresi, A.A. Heat transfer in freeze-drying apparatus. In: *Heat transfer - Book 1*; dos Santos Bernardes M.A., Ed.; InTech - Open Access Publisher: Rijeka, 2011, 91-114.

34 Liapis, A.I, Bruttini, R. A theory for the primary and secondary drying stages of the freeze-drying of pharmaceutical crystalline and amorphous solutes: comparison between experimental data and theory. Separation Technology **1994**, *4*, 144-155.

35 Sadikoglu, H, Liapis, A.I. Mathematical modelling of the primary and secondary drying stages of bulk solution freeze-drying in trays: parameter estimation and model discrimination by comparison of theoretical results with experimental data. Drying Technology **1997**, *15*, 791-810.

36 Pikal, M.J. Freeze Drying. In: *Encyclopedia of Pharmaceutical Technology*; Swarbrick, J., Ed.; Informa Healthcare: New York, 2006; 1807-1833.

37 Kessler, W.J.; Davis, S.J.; Mulhall, P.A.; Finson, M.L. System for monitoring a drying process. United States Patent No. 0208191 A1, 2006.

38 Gieseler, H.; Kessler, W.J.; Finson, M.; Davis, S.J.; Mulhall, P.A.; Bons, V.; Debo, D.J.;

Pikal, M.J. Evaluation of Tunable Diode Laser Absorption Spectroscopy for in-process water vapor mass flux measurement during freeze drying. Journal of Pharmaceutical Sciences **2007**, *96*, 1776-1793.

39 Kuu, W.Y.; Nail, S.L.; Sacha, G. Rapid determination of vial heat transfer parameters using tunable diode laser absorption spectroscopy (TDLAS) in response to step-changes in pressure set-point during freeze-drying. Journal of Pharmaceutical Sciences **2009**, *98*, 1136-1154.

40 Milton, N.; Pikal, M.J.; Roy, M.L.; Nail, S.L. Evaluation of manometric temperature measurement as a method of monitoring product temperature during lyophilisation. PDA Journal of Pharmaceutical Science and Technology **1997**, *5*, 7-16.

41 Liapis, A. I.; Sadikoglu, H. Dynamic pressure rise in the drying chamber as a remote sensing method for monitoring the temperature of the product during the primary drying stage of freeze-drying. Drying Technology **1998**, *16*, 1153-1171.

42 Chouvenc, P.; Vessot, S.; Andrieu, J.; Vacus, P. Optimization of the freeze-drying cycle: a new model for pressure rise analysis. Drying Technology **2004**, *22*, 1577-1601.

43 Velardi, S.A.; Rasetto, V.; Barresi, A.A. Dynamic Parameters Estimation Method: advanced Manometric Temperature Measurement approach for freeze-drying monitoring of pharmaceutical. Industrial Engineering Chemistry Research **2008**, *47*, 8445-8457.

44 Fissore, D.; Pisano, R.; Barresi, A.A. On the methods based on the Pressure Rise Test for monitoring a freeze-drying process. Drying Technology **2011**, *29*, 73-90.

45 Fissore, D.; Pisano, R.; Barresi A.A. Monitoring of the secondary drying in freeze-drying of pharmaceuticals. Journal of Pharmaceutical Sciences **2011**, *100*, 732-742.

46 Fissore, D.; Barresi, A.A.; Pisano R. Method for monitoring the secondary drying in a freeze-drying process. United States Patent Application: US 2010018073 (A1), 2010.

47 Hancock, B.C.; Zografi, G. The relationship between the glass transition temperature and the water content of amorphous pharmaceutical solids. Pharmaceutical Research **1994**, *11*, 471-477.

48 Barresi, A.A.; Pisano, R.; Fissore, D.; Rasetto, V.; Velardi, S.A.; Vallan, A.; Parvis, M.; Galan, M. Monitoring of the primary drying of a lyophilization process in vials. Chemical Engineering and Processing **2009**, *48*, 408-423.

49 Patel, S.M.; Doen, T.; Pikal, M.J. Determination of end point of primary drying in freeze-drying process control. AAPS PharmSciTech **2010**, *11*, 73-84.

List of Tables

Table 1. Characteristics of the various groups of vials considered in the experimental case study and values of the parameter C_1 used to model the dependence of K_v on P_c (C_2 = 1.4 W $m^{-2}K^{-1}Pa^{-1}$, C_3 = 0.02 Pa^{-1}).

List of Figures

Figure 1. Values of the heat transfer coefficient K_v for the vials of the batch (P_c = 5 Pa).

Figure 2. Evolution of the desorption rate *vs*. time (symbols) for different temperatures of the heating fluid (lines) when P_c = 5 Pa (solid line, ●: $T_{fluid,sp}$ = 40°C; dashed line, ■: $T_{fluid,sp}$ = 30°C; dotted line, ▲: $T_{fluid,sp}$ = 20°C).

Figure 3. Graph A: Desorption rate *vs*. residual moisture for different temperatures of the heating fluid (solid line, ●: $T_{fluid,sp}$ = 40°C; dashed line, ■: $T_{fluid,sp}$ = 30°C; dotted line, ▲: $T_{fluid,sp}$ = 20°C; P_c = 5 Pa).
Graph B: Arrhenius plot for the kinetic constant of the desorption reaction.

Figure 4. Comparison between calculated (lines) and measured (symbols) values of desorption rate (graph A), residual moisture (graph B), and product temperature (graph C) when $T_{fluid,sp}$ = 30°C and P_c = 5 Pa.

Figure 5. Graph A: Design space calculated in case $C_{s,0}$ = 6% and the target value of residual moisture is 2%.
Graph B**:** Design space calculated in case $C_{s,0}$ = 6% and the target value of ranges from 1 to 2 %.
Dashed lines are the boundary of the portion of the design space where the constraint on the maximum value of product temperature is not satisfied.

Figure 6. Spatial (graph A) and frequency (graph B) distribution of residual moisture content among the vials of the batch at the beginning of secondary drying.

Figure 7. Graph A: Influence of the value of $C_{s,0}$ (solid line: 4%, dashed line: 6%, dotted line: 8%) on the design space of the secondary drying ($C_{s,t}$ = 1%). The thick line identifies the boundary of the design space due to the constraint on product temperature.
Graph B: Influence of the value of K_v (solid line: 6.6 W $m^{-2}K^{-1}$, dashed line: 16.1 W $m^{-2}K^{-1}$, dotted line: 86.6 W $m^{-2}K^{-1}$) on the design space of the secondary drying ($C_{s,0}$ = 6%, $C_{s,t}$ = 1%).

Figure 8. Example of recipe optimization for the secondary drying step.
Graph A: evolution of the set-point of the fluid temperature (dashed line), of product temperature (solid line), and of the limit product temperature (dotted line) *vs*. time.
Graph B: evolution of desorption rate *vs*. time.
Graph C: evolution of residual moisture *vs*. time.

Figure 9. Comparison between the evolutions of product temperature (graph B) and residual moisture (graph C) for different heating strategies (graph A). The dash-dotted line in graph C indicates the target value for the residual moisture.

Table 1

	Position over the shelf	Additional mechanisms to heat transfer			C_1, W K^{-1} m^{-2}
		radiation from chamber walls	*contact with the metal frame*	*contact with "hot" vials*	
group 1	peripheral	yes	yes	yes	21.9
group 2	peripheral	yes	no	yes	13.6
group 3	core	no	no	yes	9.7
group 4	core	no	no	no	7.8

Figure 1

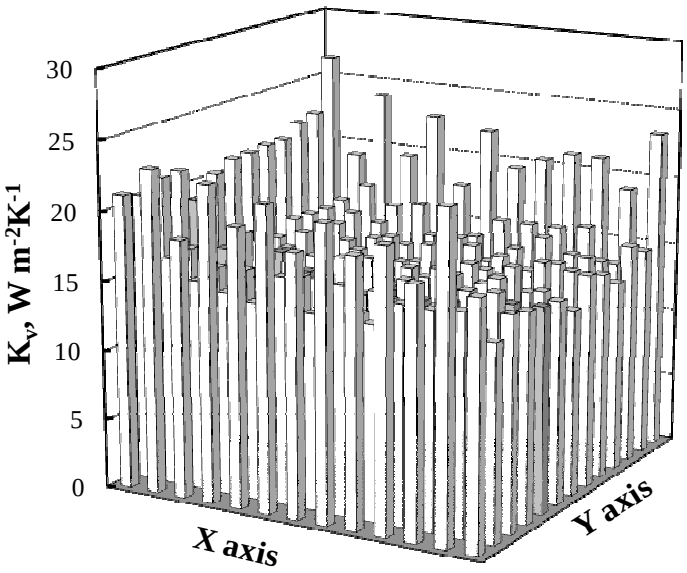

Figure 2

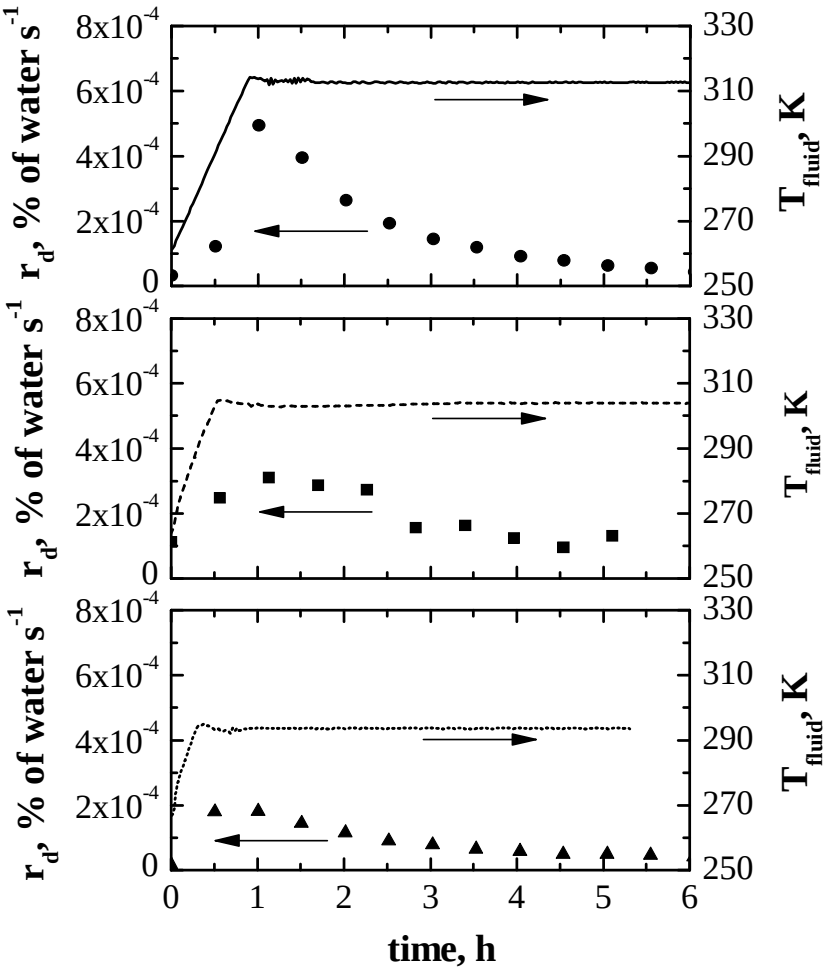
8x10-4
6x10-4
4x10-4
2x10-4
0
330
310
290
270
250
rd, % of water s-1
Tfluid, K
0
1
2
3
4
5
6
time, h

Figure 3

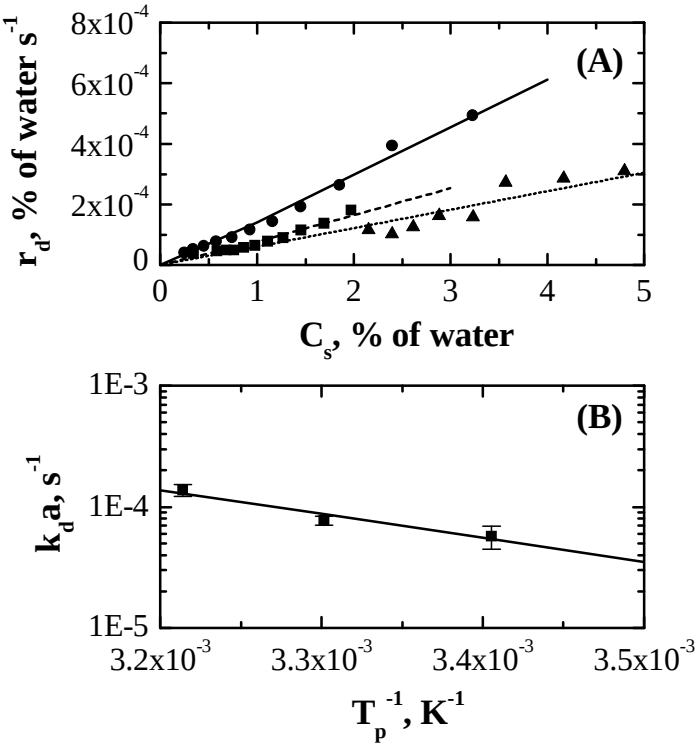
(A)
8x10-4
6x10-4
4x10-4
2x10-4
0
rd, % of water s-1
0
1
2
3
4
5
Cs, % of water
(B)
1E-3
1E-4
1E-5
kda, s-1
3.2x10-3
3.3x10-3
3.4x10-3
3.5x10-3
Tp-1, K-1

Figure 4

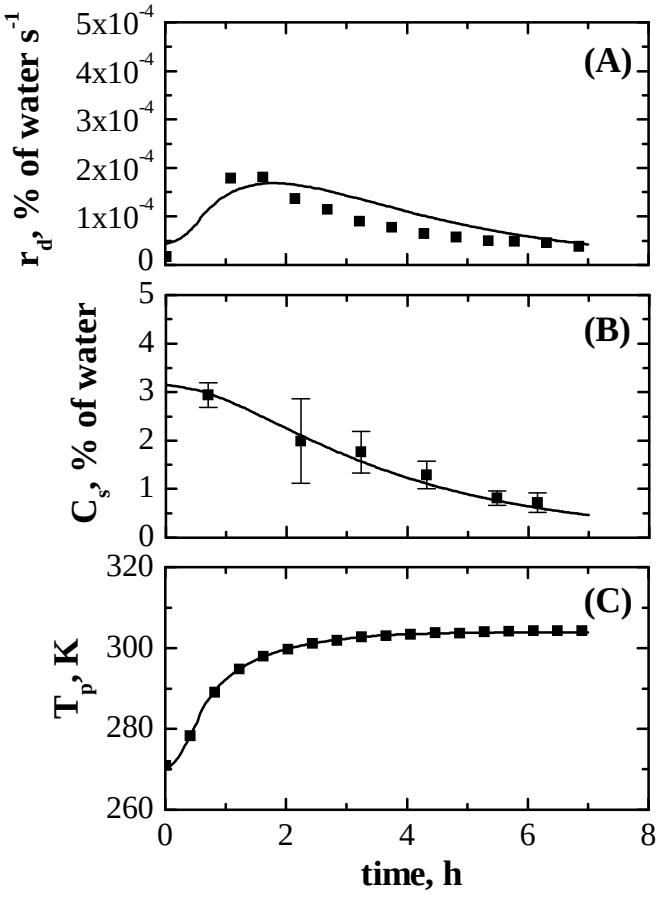
r_d, % of water s^{-1}
5x10^{-4}
4x10^{-4}
3x10^{-4}
2x10^{-4}
1x10^{-4}
0
(A)
C_s, % of water
5
4
3
2
1
0
(B)
T_p, K
320
300
280
260
(C)
0
2
4
6
8
time, h

Figure 5

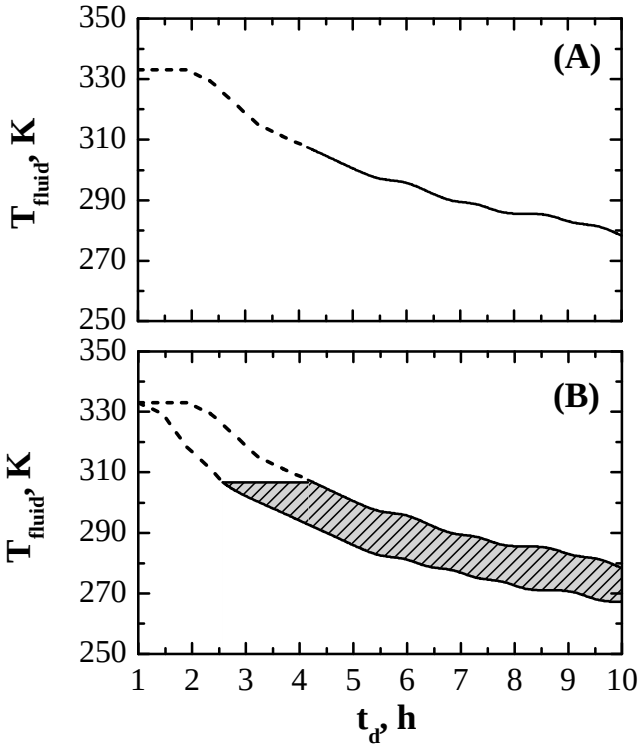

Figure 6

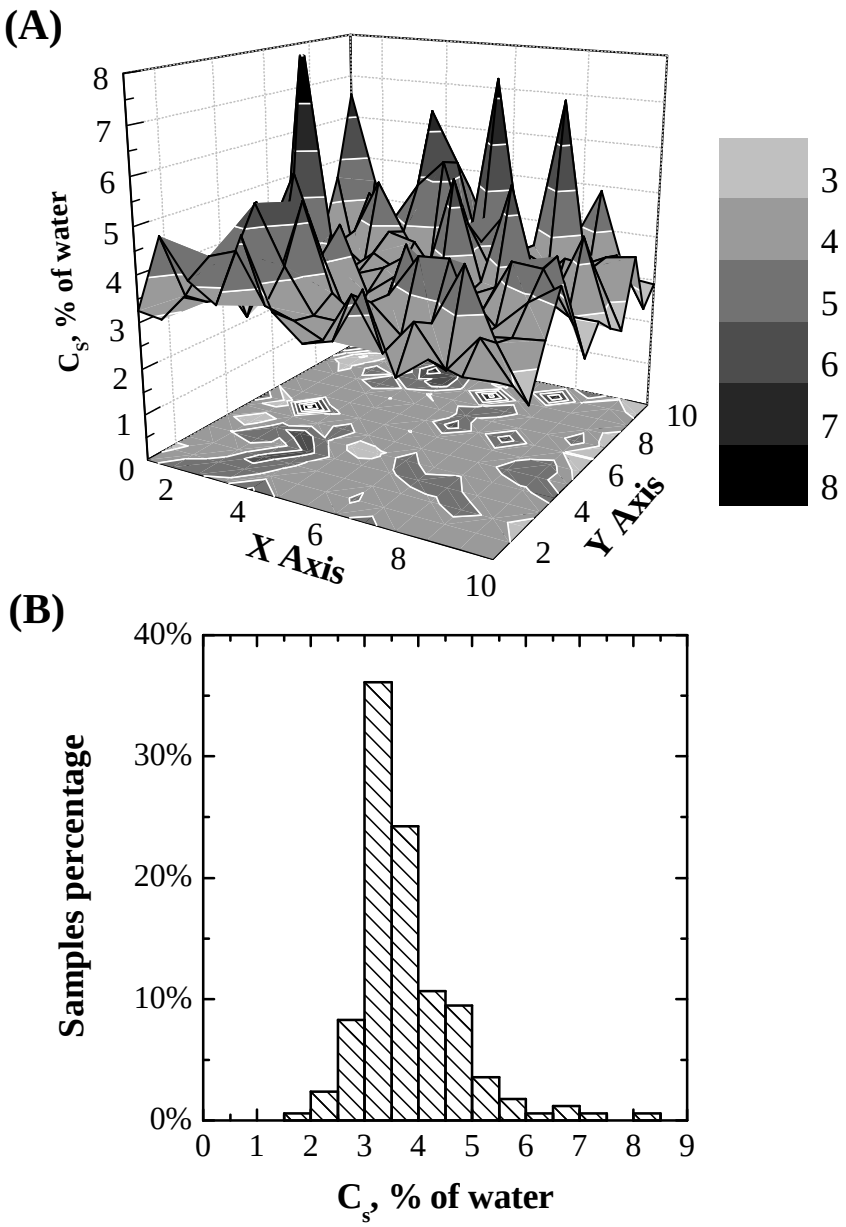

Figure 7

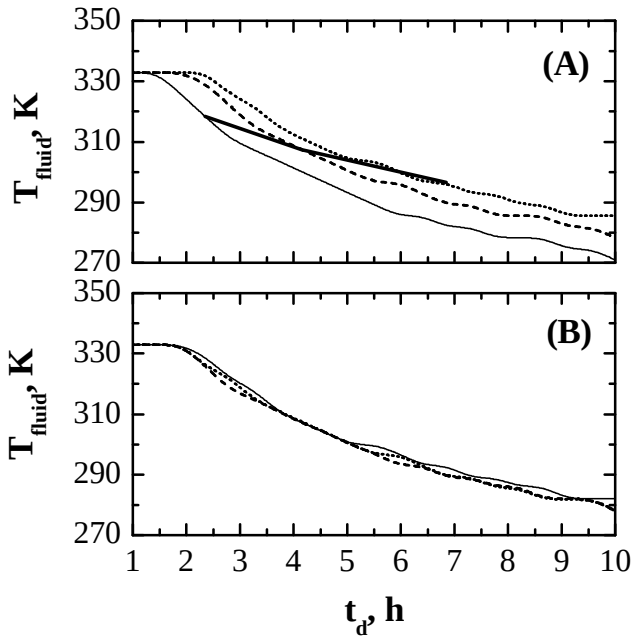

Figure 8

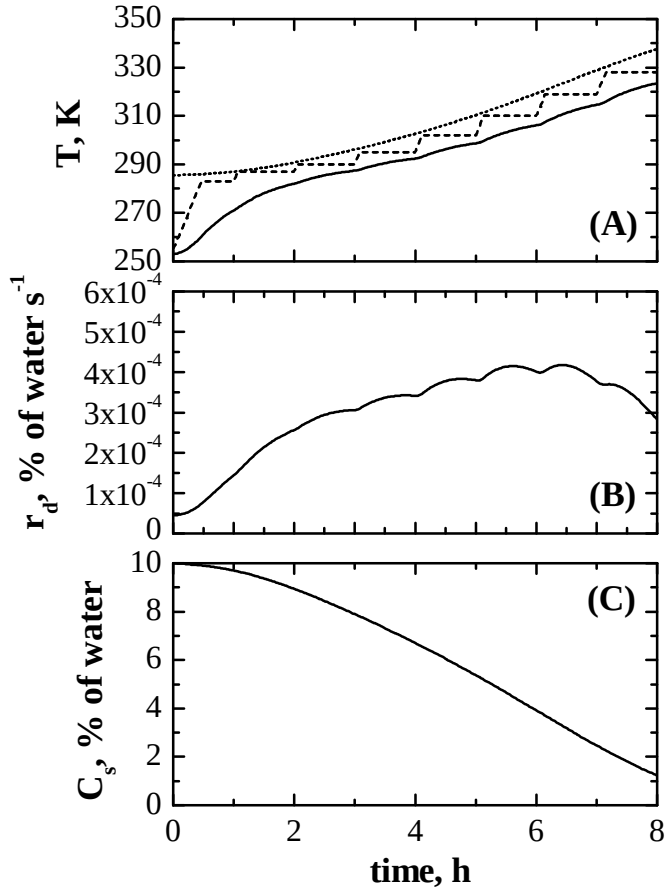
T, K
350
330
310
290
270
250
(A)
r_d, % of water s^{-1}
6x10^{-4}
5x10^{-4}
4x10^{-4}
3x10^{-4}
2x10^{-4}
1x10^{-4}
0
(B)
C_s, % of water
10
8
6
4
2
0
(C)
0
2
4
6
8
time, h

Figure 9

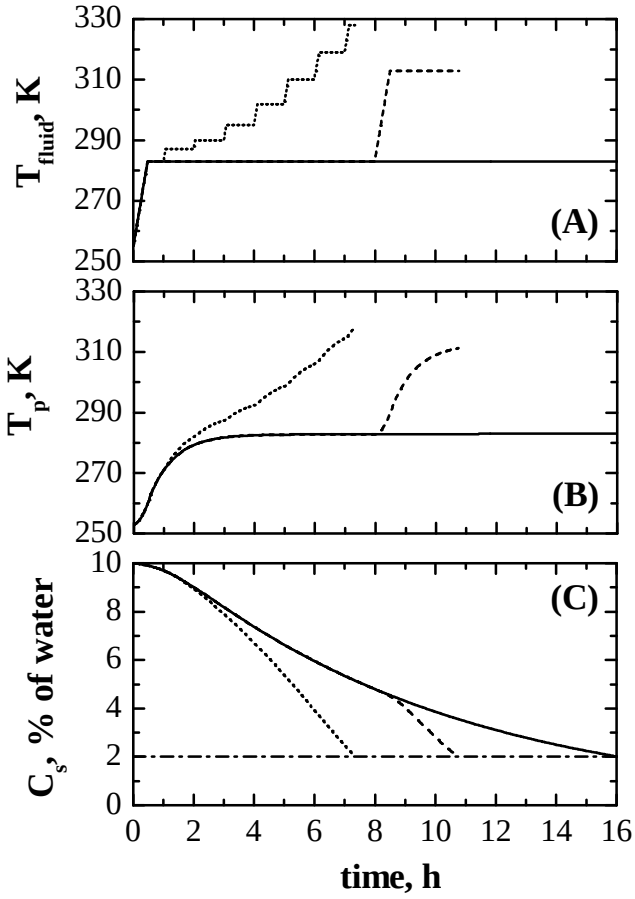
330
310
290
270
250
T_{fluid}, K
(A)
330
310
290
270
250
T_p, K
(B)
10
8
6
4
2
0
C_s, % of water
(C)
0
2
4
6
8
10
12
14
16
time, h